Molecular Coupling between Voltage Sensor and Pore Opening in the *Arabidopsis* Inward Rectifier K$^+$ Channel KAT1

RAMON LATORRE,[1,2] RICCARDO OLCESE,[3] CLAUDIA BASSO,[4] CARLOS GONZALEZ,[1,2] FABIAN MUÑOZ,[1] DIEGO COSMELLI,[1] and OSVALDO ALVAREZ[1,2]

[1]Laboratory of Biophysics and Molecular Physiology, Centro de Estudios Científicos, Valdivia, Chile
[2]Department of Biology Faculty of Sciences, University of Chile Santiago, Chile
[3]Department of Anesthesiology, Division of Molecular Medicine, and Brain Research Institute, David Geffen School of Medicine, University of California at Los Angeles, Los Angeles, CA 90095
[4]Biomedical Sciences Institute Faculty of Medicine, University of Chile, Casilla 70058, Santiago-7, Chile

ABSTRACT Animal and plant voltage-gated ion channels share a common architecture. They are made up of four subunits and the positive charges on helical S4 segments of the protein in animal K$^+$ channels are the main voltage-sensing elements. The KAT1 channel cloned from Arabidopsis *thaliana,* despite its structural similarity to animal outward rectifier K$^+$ channels is, however, an inward rectifier. Here we detected KAT1-gating currents due to the existence of an intrinsic voltage sensor in this channel. The measured gating currents evoked in response to hyperpolarizing voltage steps consist of a very fast ($\tau = 318 \pm 34$ μs at -180 mV) and a slower component (4.5 ± 0.5 ms at -180 mV) representing charge moved when most channels are closed. The observed gating currents precede in time the ionic currents and they are measurable at voltages (less than or equal to -60) at which the channel open probability is negligible ($\approx 10^{-4}$). These two observations, together with the fact that there is a delay in the onset of the ionic currents, indicate that gating charge transits between several closed states before the KAT1 channel opens. To gain insight into the molecular mechanisms that give rise to the gating currents and lead to channel opening, we probed external accessibility of S4 domain residues to methanethiosulfonate-ethyltrimethylammonium (MTSET) in both closed and open cysteine-substituted KAT1 channels. The results demonstrate that the putative voltage–sensing charges of S4 move inward when the KAT1 channels open.

KEY WORDS: KAT1 channels • inward rectifier • gating currents • cysteine accessibility • voltage sensor

INTRODUCTION

In plants, voltage-dependent K$^+$ channels are crucial for the absorption of K$^+$ from the soil and for stomatal movements (Maatuis et al., 1997). These *Shaker*-like K$^+$ channels belong to the S4 superfamily and are made up of four subunits, each of which contains six transmembrane domains (Anderson et al., 1992; Sentenac et al., 1992; Cherel et al., 1996; Urbach et al., 2000). The inward rectifiers KAT1 and AKT1 were the first inward rectifiers K$^+$ channels cloned from the plant *Arabidopsis thaliana* (Anderson et al., 1992; Sentenac et al., 1992). When expressed in *Xenopus* oocytes a time-dependent increase in current is observed upon hyperpolarization (Schachtman et al., 1992; Hoshi, 1995; Latorre et al., 2003*)*. Plant inward rectifiers are structurally similar to depolarization-activated K$^+$ channels in animals, such as the *Shaker* K$^+$ channel, for example.

Moreover, KAT1 is inserted in the plasma membrane with the same membrane topology as the one predicted for the *Shaker* channel (i.e., cytoplasmic NH$_2$ and COOH terminus of the channel-forming protein; Shih and Goldin, 1997; Uozomi et al., 1998; Sato et al., 2003). The KAT1 inward rectification does not depend on the external K$^+$ concentration or on amino acid residues that determine C-type inactivation in *Shaker* channels (Marten and Hoshi, 1998). Therefore, the inward rectifier characteristic of KAT1 is not a consequence of recovery from inactivation as was observed for HERG channel currents (Schonherr and Heinemann, 1996; Smith et al., 1996).

In KAT1, the S4 domain contains conserved, regularly spaced, and positively charged amino acids. The fact that neutralization of arginine 176 in the S4 motif of KAT1 reduces the number of apparent gating charges (Marten and Hoshi, 1998; Zei and Aldrich, 1998) suggests that the S4 motif acts as a voltage-sensing element. Neutralization of a charged residue of the

---

Diego Cosmelli's present address is LENA, CNRS UPR 640, Laboratoire de Neurosciences Cognitives et Imagerie Cérébrale Hôpital de la Salptrière, 47 Bd de l'Hôpital, 7565, Paris cedex 13, France.

Address correspondence to Dr. Ramon Latorre Laboratory of Biophysics and Molecular Physiology Centro de Estudios Científicos Arturo Prat 514 Valdivia, Chile. Fax: (56) 63-234515; email: ramon@cecs.cl

---

Abbreviations used in this paper: DTT, dithiothreitol; HCN, hyperpolarization-activated cyclic nucleotide gated; HERG, human ether a go go related gene; MTSET, trimethylammoniumethylmethanethiosulfonate.

S4 segment in the KST1 channel (R181Q) also leads to a decrease in equivalent charge movement, suggesting that in this regard KAT1 homologue S4 is also a voltage-sensing element (Hoth et al., 1997).

In animal outward rectifiers such as K^+ and Na^+ channels the main voltage sensor is the positively charged fourth (S4) transmembrane domains. This is supported by several different lines of experimental evidence. First, neutralizing the positive charges in the S4 reduces the number of gating charges coupled to pore opening (Aggarwal and MacKinnon, 1996; Seoh et al., 1996). Second, cysteine-scanning mutagenesis showed that the accessibility of S4 amino acid residues to organic ions like methanethiosulfonate-ethyltrimethylammonium (MTSET) is channel state dependent (Yang and Horn, 1995; Larsson et al., 1996; Mannuzzu et al., 1996; Yang et al., 1996). These results are strong evidence that the voltage-sensing charges contained in the S4 move outward when the channels open. Third, histidine-scanning mutagenesis showed that four of the seven positively charged residues contained in S4 of *Shaker* channels move from the cytoplasmic to the external side of the membrane during channel activation (Starace and Bezanilla, 2001). This accounts for the steepness of the voltage-activation curve, as it indicates the presence of three to four charges per voltage sensor (for reviews see Sigworth, 1994; Yellen 1998; Bezanilla, 2000). More recently, Jiang et al. (2003a,b) elucidated the crystal structure of a bacterial voltage-dependent K^+ channel (KvAP) and proposed a mechanism for the gating charge movement. The experiments of Jiang et al. (2003a,b) indicate that in KvAP channels the S4 and a portion of the S3 (S3b) segment form a "paddle". The paddles of each subunit are located near the intracellular surface when the channel is closed and are displaced from the inside to outside when the channel opens. Assuming a membrane thickness of 35 Å, the distance traveled by the paddles is of the order of 20 Å (compare Bezanilla, 2000).

With a conserved S4 segment, this domain may function in KAT1 as a voltage sensor that couples membrane hyperpolarization with channel opening. In a preliminary communication (Cosmelli et al., 2000), based on gating current measurements and cysteine scanning mutagenesis, we proposed that KAT1 possesses an intrinsic voltage sensor and that sensor displacement, which leads to channel opening, is inward. This was confirmed by studies in two closely related hyperpolarization-activated ion channels, the cyclic nucleotide–gated (HCN) cation channel (Männikö et al. 2002) and in a Methanococcal voltage–gated K^+ channel (Sesti et al., 2003).

The purpose of this study is: (a) to give a detailed characterization of KAT1-induced gating currents, and (b) to determine the external accessibility of the S4 amino acid residues to the membrane-impermeant thiol reagent MTSET in both open and closed states using cysteine-substituted KAT1 K^+ channels. Our results show that the S4 domain functions as the voltage sensor in KAT1 channels and that residues located beyond arginine 176 toward the S4 carboxyl terminus become inaccessible from the external milieu to the MTSET when the channel is open. These experiments indicate that in KAT1, as opposed to *Shaker* K^+ channels, the inward displacement of the voltage sensor leads to channel opening. This difference between *Shaker* and KAT1 channels must reside in the coupling of the voltage-sensor movement to the activation gate.

MATERIALS AND METHODS

Molecular Biology

The KAT1 cDNA was provided by the laboratory of Dr. Franco Conti (National Research Council, Genova, Italy). The KAT1 K^+ channel–coding region from pGEMHE was transferred to pALTER (Promega) for the generation of oligonucleotide-directed mutants. Whole plasmids with their inserts were synthesized and ligated (looping in). DNAs were sequenced along the stretch of interest flanked by two single-cut restriction enzymes. Plasmid DNA was linearized with NheI and RNA was transcribed in vitro using the T7 mMESSAGE mMACHINE kit (Ambion). The mRNA was dissolved in water to a final concentration of 0.5 µg/µL. Stage IV-V oocytes were removed from adult female *Xenopus laevis* frogs and incubated in ND-96 media as described (Gonzalez et al., 2001). 5–50 ng of mRNA solution in 50 nL of water were injected into each oocyte and stored at 18°C.

Electrophysiology

After 2–4 d of mRNA injection, macroscopic and gating currents induced by the expression of KAT1 or mutant channels in the membrane of the oocytes were recorded using the cut-open oocyte voltage clamp (Taglialatela et al., 1992). Since this technique has not been used previously to characterize KAT1 electrophysiology, the data obtained with it was checked for the wild-type and mutant channels using the macropatch technique. The extracellular solution contained (in mM) 110 K-MES, 2 CaCl$_2$, 10 HEPES, pH 7.4. The intracellular solution contained (in mM) 110 K-MES, 2 EDTA, 10 HEPES, pH 7.4. To record gating currents K^+ was replaced by NMG and 0.1 mM ouabain was added to the solution in order to inhibit the gating currents originated by the Na^+/K^+ pump. The microelectrode used to measure the membrane voltage contained: 2.7 M Na-MES, 10 mM NaCl, 10 mM HEPES, pH 7.0. Microelectrode resistance was 100–300 kΩ. The linear capacitive and the leak currents were subtracted with small positive pulses (P/4) of 1/4 the test pulse amplitude from a subtracting holding potential of 0 mV. When measuring gating currents the data was filtered with a 5- or 10-kHz low pass 8-pole Bessel filter. Data were acquired at a frequency fivefold faster than the filtering frequency.

Ionic currents were usually acquired at 1 kHz and filtered at 200 Hz. The conductance-voltage curve was obtained using tail current measurements. The tail currents were fitted with a single exponential and the time zero amplitudes were extrapolated.

Normalized conductance, G/G_{max} data were fitted using a Boltzmann function:

$$\frac{G}{G_{max}} = \frac{1}{1 + \exp[-zF(V - V_{1/2 - G})/RT]}, \quad (1)$$

where F, R, and T have their usual meanings, z is the equivalent gating charge per channel, V is the membrane voltage, and $V_{1/2 - G}$ is the voltage where the Boltzmann distribution is equal to $1/2$. Normalized charge Q data were fitted using a Boltzmann function:

$$\frac{Q}{Q_{max}} = \frac{1}{1 + \exp[-z_g F(V - V_{1/2 - Q})/RT]}, \quad (2)$$

where z_g is the equivalent gating charge per voltage sensor and $V_{1/2Q}$ is the voltage where the Boltzmann distribution is equal to $1/2$.

Alternatively, macroscopic currents were recorded in cell-attached macropatches of oocyte membrane. Patch pipettes of 30–70 μm had a resistance of ∼0.2 MΩ. Bath and pipette solutions were (in mM) 110 K-MES, 2 CaCl$_2$, 10 HEPES, pH 7.4. The acquisition and basic analysis of the data were performed with PCLAMP 6.0 software (Axon Instruments, Inc.) driving a 12-bit analogue interface card.

MTSET Labeling

Labeling of channel to MTSET was performed by superfusion of the oocyte under cut-open oocyte voltage clamp. The MTSET solution was prepared freshly by directly dissolving the compound in the external solution to a final concentration of 4 mM. Antioxidant dithiothreitol (DTT) was used in all the MTSET labeling experiments. We followed the time course of channel modification by recording every 6 s the ionic current responses to 300 ms or 1 s −160-mV pulses maintaining a constant holding potential during the intervals. Holding potentials were 0 mV for the closed protocol and −140 mV for the open/closed protocol. In all of the cysteine substituted channels, labeling followed a monoexponential time course. From the time constants of the exponentials the second order rate constant (M^{-1}s^{-1}) was extracted providing a measure of cysteine exposure in the closed and open configurations of the channel. MTSET did not modify the electrophysiological characteristics of wt KAT1 channels.

RESULTS

Voltage-dependent Activation

KAT1-gating currents were detected by maximizing the expression of KAT1 channels as shown in Fig. 1, which displays representative examples of KAT1 ionic currents measured using symmetrical 110 mM K$^+$ methanesulfonate (KMES; Fig. 1 A). Only experiments in which the ionic currents were larger than 25 μA at −160 mV were used for gating current experiments. Fig. 1 B displays the logarithm of the relative conductance-voltage [G/G_{max} − V] curve obtained from the tail currents (Fig. 1 B, inset). The best fit to the G/G_{max} − V data shown in Fig. 1 B using a Boltzmann function (Eq. 1) was obtained with half activation voltage, $V_{1/2 - G} = -139$ mV and $z = 1.31$ (average values were $V_{1/2 - G} = -148 \pm 3$ mV and $z = 1.2 \pm 0.06$, $n = 13$). Using the macropatch technique (cell-attached configuration) to measure KAT1-induced ionic currents the values for $V_{1/2 - G}$ and z were -145 ± 4 mV and 1.1 ± 0.1, respec-
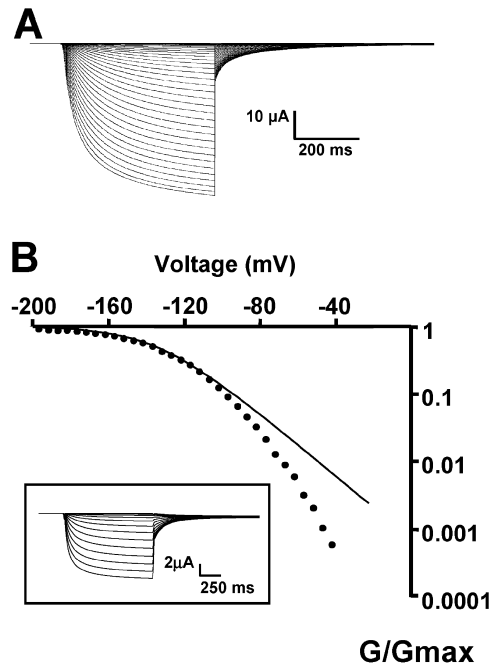

FIGURE 1. KAT1 ionic currents recorded using the cut-open oocyte voltage clamp technique under symmetric 110 mM KMES. (A) KAT1 ionic currents were recorded in response to 1-s voltage steps from −85 to −250 mV in 5-mV increments followed by a step to −40 mV. Holding potential was 0 mV. This is the amount of KAT1 channel expression needed to detect KAT1 gating currents as described in the text. (B) Voltage dependence of the activation of KAT1 channels. The conductance-voltage curves were obtained using tail current measurements (inset). Solid line is a fit to the normalized conductance (G/G_{max}) − V data to a Boltzmann function as explained in MATERIALS AND METHODS. $V_{1/2\text{-}G} = -139$ mV and $z_G = 1.31$.

tively ($n = 4$). These values are in reasonable agreement with others published previously (e.g., Hedrich et al., 1995; Hoshi, 1995). Notice that a simple Boltzmann (Eq. 1; Fig. 1 B, line) fails to fit the G-V data at low open probabilities, implying that this type of fitting underestimates the actual number of equivalent gating charges. Limiting slope analysis, a method developed by Almers (1978) and generalized by Sigg and Bezanilla (1997) gives the number of equivalent charges coupled to the channel opening for sequential or nonsequential models with any number of closed or open states as long as the transitions between open states are voltage independent. We have determined the limiting slope at open probabilities ≤10^{-3} from experiments like the one depicted in Fig. 1 B and extracted from it the number of equivalent charges, $z_{lim} = 2.6 \pm 0.3$ ($n = 7$). To increase the voltage resolution, we used slow ramp simulation from −120 to 0 mV (Fig. 2; Noceti et al., 1996; Seoh et al., 1996; Gonzalez et al., 2000). The steady-state conditions were checked by varying the speed of the ramp and by testing the symmetry of the current in response to a symmetric triangular voltage wave. The

A

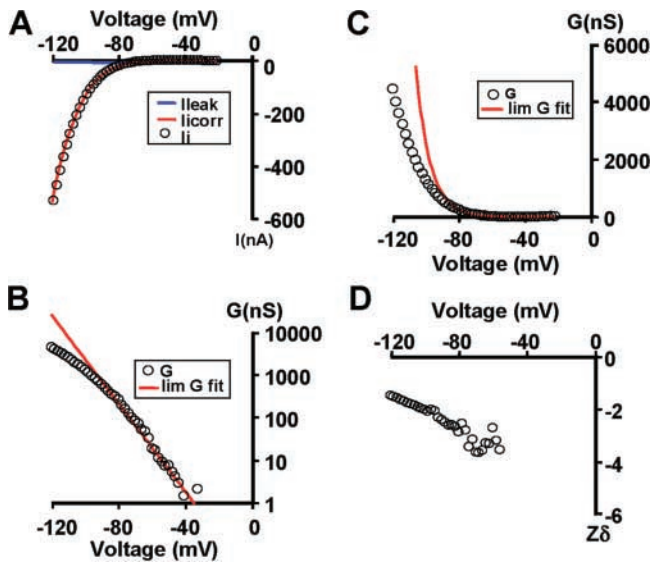Voltage (mV)

B

C

G(nS)

D

Voltage (mV)

FIGURE 2. Limiting slope analysis in KAT1 channel. (A) Ionic currents recorded with the cut-open oocyte technique. Slow depolarization with a voltage ramp from -20 to -120 mV. The ionic currents showed in the figure is the average of 10 voltage ramps. Linear leakage correction was performed off line using a linear fit to the points at potentials more positive than -40 mV. Data points were decimated average of five points. (B) *G-V* relationship (open circles) in a linear plot. Data points between -20 and -80 mV were fitted to Eq. 3 solid red line. The fitted parameters were A = 23 nS and $z_{\lim}^{ramp}$ = 2.9 . (C) *G-V* curve a fitted limiting slope (solid red line) in a semilog scale. (D) Relationship between the calculated gating charge, *z*, and potential, *Em. z* was calculated as $z = \dfrac{RT}{F}\dfrac{d\ln G}{dV}$.

leakage current was fit to a straight line and was subtracted from the record to obtain the ionic current (Fig. 2 A). This method is adequate for obtaining a quasi-steady-state *G-V* relationship at potentials greater than -40 mV (Fig. 2 C). The G-V plot was fitted to a monoexponential approximation (red solid line) in the limit of small negative voltages (Fig. 2 B):

$$G(V) = Ae^{z_{\lim}^{ramp}FV/RT}, \qquad (3)$$

where *A* is a constant and $z_{\lim}^{ramp}$ is the effective charges per channel obtained with the ramp method. The G_{max} in this particular experiment was 40 µS and, therefore, the ramp method allowed us to determine the limiting slope at open probabilities $>10^{-4}$. The average $z_{\lim}^{ramp}$ was 3.0 ± 0.2 ($n = 5$). Assuming a tetrameric structure for KAT1 of four independent subunits, these results imply that $\sim$0.75 electronic charges per sensor move the whole electric field during channel opening. $z_{\lim}^{ramp}$, however, should be considered a lower limit of the number of gating charges per channel since a plot of *z* as a function of voltage does not show a clear voltage-independent value for *z* (Fig. 2 D; Zagotta et al., 1994; Noceti et al., 1996; Seoh et al., 1996; Gonzalez et al., 2000, 2001).

KAT1 Gating Currents Revealed

Gating currents from KAT1 were successfully recorded using the cut-open oocyte voltage clamp technique (Taglialatela et al., 1992) after maximizing the level of expression. The fast transient current observed at the ON and the OFF of the voltage pulses on Fig. 3, A and B, respectively, are the KAT1 gating currents. These transient currents were absent in oocytes not injected with KAT1 mRNA or injected with water (unpublished data). In Fig. 3 A, we replaced K^+ in the internal compartment by NMG, and reduced the external K^+ concentration to 10 mM. In Fig. 3 A we also increase the current and time scale in order to unveil the ON gating currents (I_{gON}) and to compare the time courses of I_{gON} with those of the ionic currents. Notice in Fig. 3 A that: (a) gating currents are fast and precede ionic currents at small negative voltages; (b) ionic current activation is clearly sigmoid; and (c) measurable gating currents appear at smaller hyperpolarizing voltages than the ionic currents. At larger negative voltages, after the initial component of the gating current, the onset of the ionic currents overlaps the decay of the gating currents. These observations suggest the presence of several closed states through which there is fast transit of charge before channel opening, and that transitions between closed and open states should be slow or rate limiting. More important, the results depicted in Fig. 3, A and B, are a clear indication that KAT1 channels contain an intrinsic voltage sensor.

The gating current was observed by replacing internal and external K^+ by NMG (Fig. 3 B). Gating currents are fast transient currents with biexponential decays with time constants at the ON (of a voltage step) of 318 ± 34 µs and 4.5 ms $\pm$ 0.5 ($n = 3$, -180 mV). An example of the goodness of the biexponential fit is shown in Fig. 3 C. Since the fast component of Ig_{ON} is orders of magnitude faster than the ionic current activation constant, this fast component represents activation of voltage sensors from a resting to an activated state while channels are closed. The decay of I_{gOFF} can be well fit by double-exponential functions with time constants of 397 ± 103 µs and 4.1 ± 0.6 ms at -180 mV ($n = 3$) (Fig. 3 D).

The time course of the macroscopic K^+ current (I_K) is well described by a delay followed by an exponential time course indicating that the kinetics of voltage activation are dominated by a rate-limiting transition (Schoppa and Sigworth, 1998). For mSlo channels the kinetics of the slow gating charge (Q_{slow}) movement and I_K relaxation are similar, suggesting that Q_{slow} also reflects this rate-limiting step. For KAT1 channels, however, the situation is different since the time constant obtained from Fig. 3 C for Q_{slow} is 4.5 ± 0.5 ms ($n = 3$) and for I_K is 122 ± 19 ms at -180 mV ($n = 6$). This result suggests that in KAT1 channels Q_{slow} represent charge movement between channel states not related with the rate-limiting
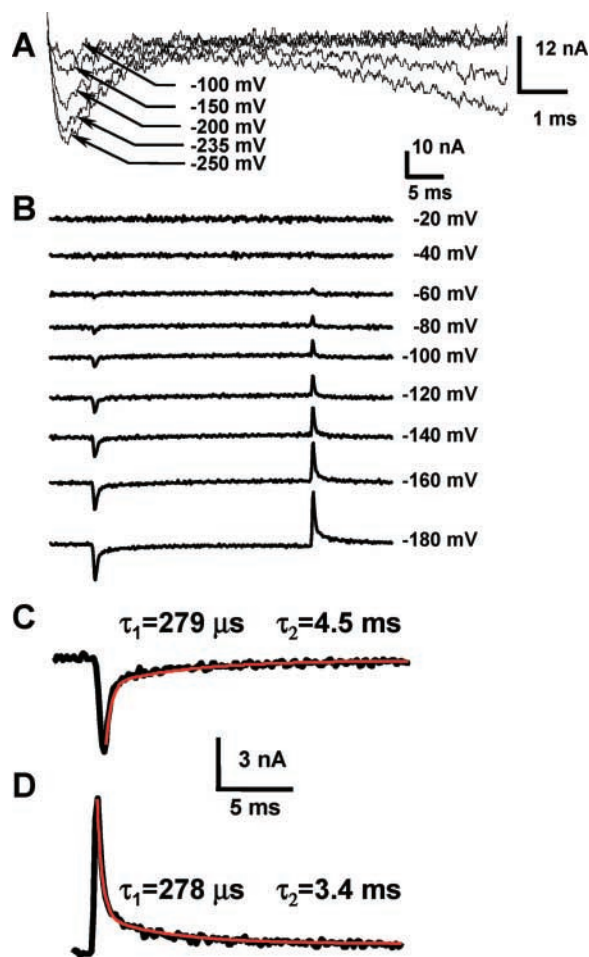
Figure 3. Gating currents induced by KAT1 channels. (A) Gating and ionic currents recorded in K$^+$-free internal solution, 10 mM external K$^+$, after a step depolarization to the indicated voltages. Holding potential was 0 mV. (B) A family of gating current records evoked in response to 30-ms voltage pulses, from a holding potential of 0 mV, in K$^+$-free solutions. Notice that gating currents are apparent at -60 mV, a voltage at which the probability of opening is <0.01 (see Fig. 1 B). (C) ON gating currents measured at -180 mV, red line is a biexponential fit with the indicated fast and slow time constants. (D) OFF gating currents measured at 0 mV, after a 30 ms -180 mV pulse. Red line is a biexponential fit with the indicated fast and slow time constants.
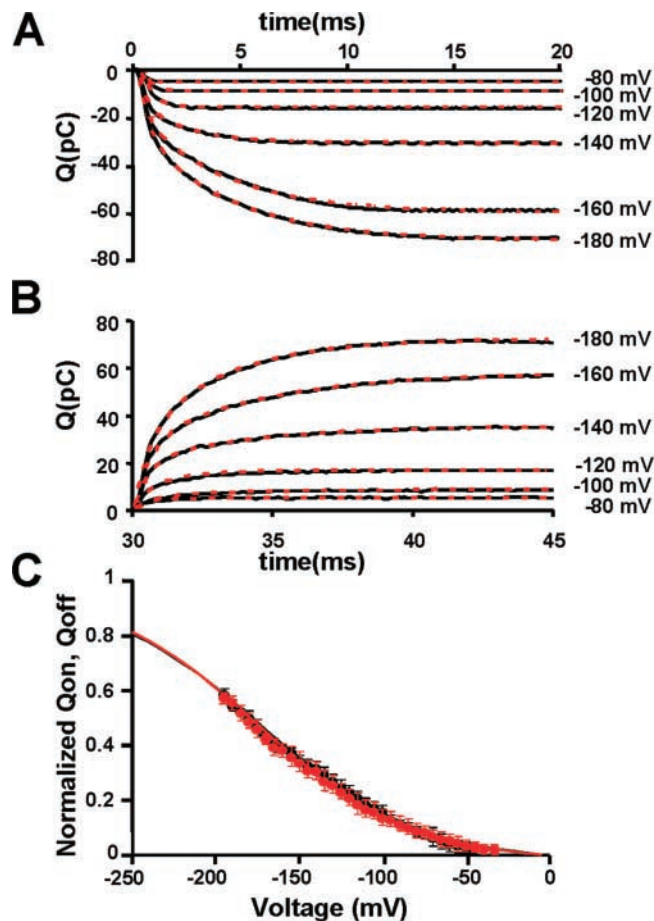

Figure 4. Properties of KAT1 gating currents. (A) Gating charge calculated as the time integral of the ON gating currents shown in Fig. 3 B. (B) Gating charge calculated as the time integral of the OFF gating currents shown in Fig. 3 B. Between -80 and -120 mV the gating charge time course is well described by a single exponential fit with a time constant of the order of 300 µs. Between -140 and -180 mV, a biexponential fit is necessary to account for the gating charge time course. (C) Comparison between normalized Q_{ON} and Q_{OFF}. Data was fitted using Eq. 2 with: $z_{g - ON} = 0.56 \pm 0.10$, $V_{1/2 - QON} = -176 \pm 9$ mV; $z_{g - OFF} = 0.57 \pm 0.15$, $V_{1/2 - QOFF} = -172 \pm 10$ mV ($n = 5$).

step that determines the time course of I_K. If this is the case, Q_{slow} should represent charge displacement between closed states. This conclusion is further corroborated by inspecting the current traces of Fig. 3 A. In this particular oocyte, after 10 ms, I_K increases to 0.2% of the steady-state amplitude, representing at -250 mV only 0.19% of maximum P_0. Therefore, the slow component of the gating charge we observe is associated with events preceding channel opening.

The time integrals of I_{gON} and I_{gOFF} are shown in Fig. 4 A. Q_{ON} increases with a time course that can be fitted by a fast phase corresponding to the rapid decay of I_{gON}, and a slow component that becomes apparent at potentials more negative than -140 mV. This slow component relaxes with a time constant of 4.2 ms at -180 mV and represents a significant fraction (65%) of the total charge movement. The Q_{ON}(V) and Q_{OFF}(V) relationships are plotted in Fig. 4 C. We notice that if the time integral of the ON gating current is performed over a time span of 30 ms the amount of charge moved at the ON is recovered at the end of the pulse over the range of hyperpolarizations we explored (Fig. 4 C, $n = 5$) (compare legend for Fig. 4 C).

In Fig. 5 each point represents measurements of ionic conductance and gating currents performed in the same oocyte. When comparing oocytes with different channel densities, we found that the amount of gating charge is directly proportional to the magnitude of
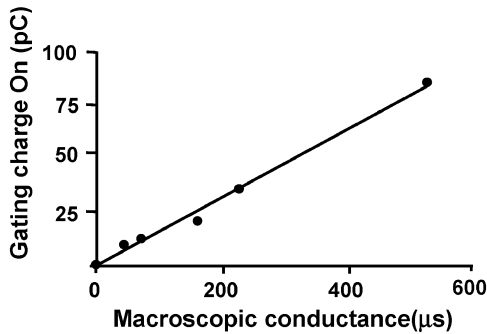
FIGURE 5. Proportionality between gating charge and KAT1-induced K^+ conductance. Each point represents a different oocyte in which the ionic conductance and gating currents were measured at -180 mV. K^+ currents were measured in the presence of 110 mM K-MES in the external side, which was subsequently replaced by 110 mM NMG-MES when measuring gating currents. Gating charge was obtained integrating I_{gON}.

KAT1-induced K^+ conductance. The data shown in Fig. 5 confirms that the fast transient current we detect at the beginning and at the end of the voltage pulse are indeed KAT1 gating currents. The channel conductance can be calculated from the z obtained using the limiting slope method and the Q-G data shown in Fig. 5. Using, for example, the measured 50 pC and a $z = 3$, this Q_{ON} would correspond to 104×10^6 channels, suggesting a 335×10^{-6} μS$/104 \times 10^6 = 3.2$ pS unitary conductance. This value is smaller than the 7.5 pS reported by Zei and Aldrich (1998), but the order of magnitude is acceptable. This calculation also supports our contention that the gating currents we recorded are actually KAT1 gating currents.

Coupling between charge movement and pore opening of KAT1 channels was analyzed constructing voltage-activation curves for both gating $[Q(V)]$ and ionic $[G(V)]$ currents (Fig. 6). For small negative voltages the $Q(V)$ curve is positive to the $G(V)$ curve but crosses it near a $G_{rel} = 0.3$ at -130 mV. The crossing over of the $Q(V)$ and $G(V)$ curves could suggest the presence of multiple open states (Stefani et al., 1997; Horrigan and Aldrich, 2002). It is possible, however, that this crossing over is the result of an underestimation of the total charge. In fact, since the close to open transition of KAT1 occur in a time scale of hundreds of milliseconds there must be a slow moving charge (indistinguishable from the baseline) that remains undetected in our experimental conditions. In fact, the $Q(V)$ curve predicted by the model of Zei and Aldrich (1998) precedes the $G(V)$ at all voltages as described by the blue dot-dashed line in Fig. 6. In principle, all the gating charge could be recovered when the voltage pulse is turned off. However, technical difficulties have hindered the possibility to perform accurate enough measurements of gating currents in the OFF of the voltage
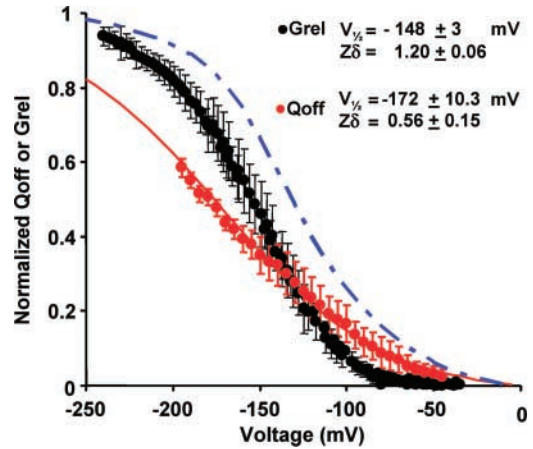

FIGURE 6. Normalized voltage-activation curves for gating (Q_{OFF}, red circles) and ionic currents (G/G_{max}, black symbols). Conductance and Q_{ON} data points were fit to Boltzmann functions as described in MATERIALS AND METHODS. $V_{1/2-G} = -148 \pm 3$ mV and $z = 1.20 \pm 0.06$ ($n = 13$). $V_{1/2-Q} = -172 \pm 10$ mV and $z_Q = 0.57 \pm 0.15$ ($n = 8$). The solid blue line is the predicted Q-V curve for the KAT1 using the voltage-dependent rate constants for Scheme I given by Zei and Aldrich (1998).

pulse that would allow us to detect the charge moved in channel transitions between closed states near the open state and in the C-O rate limiting transition. These difficulties include the need of long pulses of very large amplitudes, the small size of the gating current, and the presence of residual intracellular K^+.

State-dependent Accessibility of S4 Residues

The next question to ask was whether or not the S4 charges in KAT1 serve a voltage-sensing function. The movement of the voltage-sensing element was evaluated by substituting cysteines into the S4 segment of KAT1 channels and assaying their accessibility with MTSET (Akabas et al., 1992; Karlin and Akabas, 1998). We engineered eight individual cysteine substitutions along the length of the S4 domain (Fig. 7 A) and one near the pore region (N237C) that corresponds to the turret domain in the KscA structure (Doyle et al. 1998). The eight cysteine-substituted mutants induced robust hyperpolarizing currents at wild-type levels in *Xenopus laevis* oocytes as shown in Fig. 7 B. Among all mutants, R177C (-16 mV) and R176C ($+35$ mV) show the largest shifts of $V_{1/2}$ G-V (Fig. 7 C and Table I). Shifts of this magnitude imply that the perturbation of the free energy difference between open and closed states ($\Delta\Delta G = ze_0\Delta V_{1/2}$ where z is the equivalent gating charge and e_0 the electronic charge) introduced by the mutations is $\sim$1 kcal/mol assuming a $z = 1$ (Table I). Thus, the effects of the mutations on channel gating are modest considering that we are changing four residues, one in each subunit, of the KAT1 channel. This contrasts with the large effects observed for homologous residues in *Shaker* K^+ channels (Larsson et al., 1996).
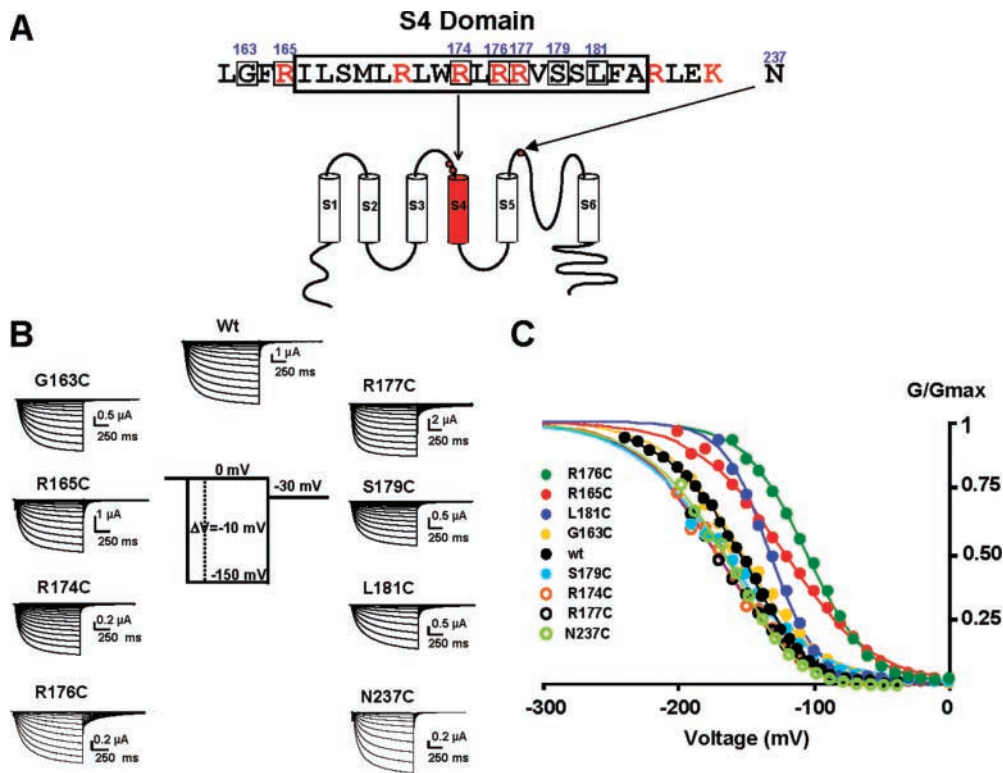
FIGURE 7. Properties of KAT1 cysteine mutants. (A) Numbered amino acid residues indicate the location of the cysteine substitutions introduced in the KAT1 protein. (B) Macroscopic currents for the different cysteine mutants. Currents were recorded using the cut-open oocyte voltage-clamp technique from oocytes expressing the different cysteine-substituted channels. (C) Normalized G/G_{max} − V relationships for the different cysteine-substituted channels. Solid lines are fit to the G/G_{max} − V data using a Boltzmann function as described in MATERIALS AND METHODS. Fitting parameters for the different mutants are given in Table I.

MTSET reacts with the sulfhydryl moiety of cysteine transferring the charged trimethylammonium-ethane-sulfide part of MTSET to the cysteine sulfide. Wild-type KAT1 channels exposed to external MTSET do not experience any detectable electrophysiological modification. When cysteines were substituted near the pore (mutant N237C) and in the S4 segment, however, large and irreversible changes in KAT1 gating were detected after external addition of the thiol reagent. The N237C mutant was used as an internal control since it is expected that residue 237 should be facing outwards in both closed and open channels. In other words, its accessibility to the thiol reagent should be independent of the state in which the channel is found. The experimental result was consistent with this prediction (unpublished data). We characterize these changes for each of the cysteine mutants by aiming to assay functionally whether a particular position was exposed in the open and or closed channels. Fig. 8, A and B, shows the voltage protocols followed to determine cysteine accessibility in the closed and in the open/closed configuration of the channel. In the closed protocol the membrane was kept at a holding potential of 0 mV and the time course of the MTSET effect was determined by applying a test voltage of −160 mV (Fig. 8 A). In the open/closed channel configuration the holding voltage was −140 mV and the test voltage −160 mV (Fig. 8 B). Fig. 8, C and D, show current records obtained before and after perfusion with MTSET outside of an oocyte expressing the G163C mutant. Externally perfused MTSET

labeled G163C in both closed and open/closed channels (Fig. 8, C and D). Fig. 8, C and D, exemplified a case of an amino acid residue that in both closed and open states faces extracellularly, as indicated by the fact that MTSET accessibility is independent of channel state.

With the exception of the wild-type channel and the L181C mutant, MTSET caused significant irreversible changes in gating. We assessed these changes by comparing current records acquired before exposure to MTSET

TABLE I

Properties of KAT-1 Cysteine Mutants and State-dependent Exposure of S4 Amino Acid Positions

| | Voltage activation | | | MTSET tagging | | | |
| | | | | Closed | | Closed/ open | |
Mutants	$V_{1/2}$	z	n	Rate constant	n	Rate constant	n
	mV			*Ms^{-1}*		*Ms^{-1}*	
G163C	−152 ± 32	1.20 ± 0.23	7	3.6 ± 0.5	3	3.7 ± 0.4	3
R165C	−126 ± 34	0.80 ± 0.14	5	7.0 ± 4.0	3	7.0 ± 2.9	3
R174C	−160 ± 20	1.29 ± 0.15	10	2.1 ± 0.5	4	5.4 ± 2.2	4
R176C	−109 ± 5.7	1.10 ± 0.1	5	4.2 ± 0.5	3	6.0 ± 0.8	3
R177C	−173 ± 17	0.90 ± 0.3	8	1.4 ± 0.4	4	NA	5
S179C	−159 ± 33	1.27 ± 0.26	8	0.96 ± 0.3	3	NA	5
L181C	−132 ± 6	1.48 ± 0.19	6	NA	3	NA	3

NA, not accessible. External closed and closed/open rates were calculated as the inverse of the time constant of modification under closed or closed/open channel perfusion with MTSET, respectively. n is the number of experiments.
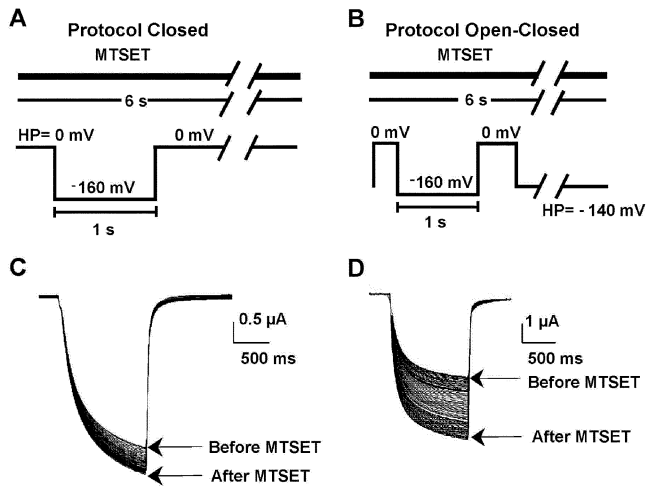
FIGURE 8. State-dependent modification of KAT1 cysteine mutants currents induced by external MTSET. (A) Voltage protocol for the assay of closed channels. The time course of channel modification was followed by recording every 6 s the ionic current responses to 300 ms or 1 s −160-mV pulses maintaining a constant holding potential during the intervals. Holding potential was 0 mV. (B) For the open-closed protocol the holding potential was −140 mV and the test pulse as in A. MTSET was superfused continuously in the assay of extracellular accessibility during cut-open oocyte voltage clamping. (C) MTSET modification of the macroscopic currents induced by the G163C mutant using the closed protocol. (D) Macroscopic currents induced by the G163C mutant before and after MTSET using the open/closed protocol.

with those acquired after MTSET wash-out. MTSET shifted the *G-V* curves in all but the L181C mutant. After exposure to MTSET the *G-V* curves for the mutants G163C and G177C shifted toward the left along the voltage axis, indicating that in these mutants, MTSET stabilized the open conformation of the channel. *G-V* curves for mutants R165C, R174C, R176C, and S179C were right-shifted after MTSET exposure, suggesting stabilization of the channel closed configuration. Surprisingly, in one mutant, R174C, we found that the *G-V* curve shift was state dependent. If the MTSET reaction was performed keeping KAT1 channels closed, the *G-V* curve was left-shifted. On the other hand, if the MTSET reaction was performed using the open/closed protocol, the *G-V* curve was right-shifted. Although the *G(V)* curves for the cysteine mutants were shifted along the voltage axis, we found that the value of *z* for the mutants was not modified after MTSET exposure (compare Männikö et al., 2002). The time course of the ionic current modification after exposure to MTSET was well described by a single exponential function (Fig. 9). The inverse of the fitted time constant provides the second order rate constants, k_c and $k_{c/o}$ in $M^{-1}s^{-1}$, which are estimates of the cysteine accessibility in the closed and open configurations, respectively (Table I). As cysteine 163, cysteines 165, 174, and 176 are also accessible from the extracellular side in both closed and open/closed channels (Fig. 9, B–D, respec-
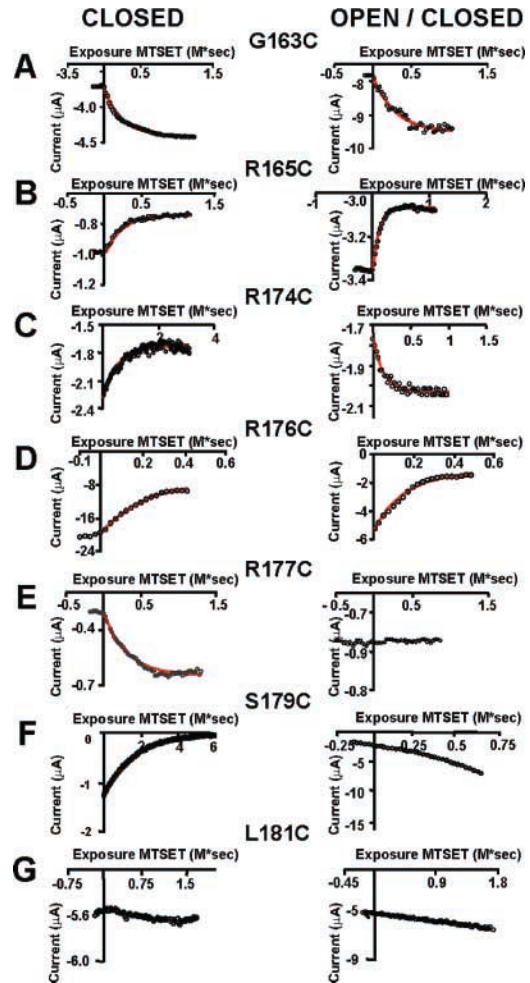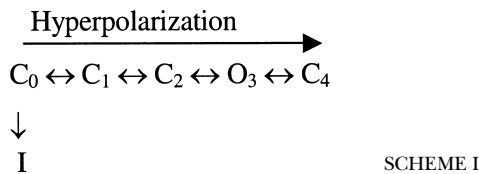

FIGURE 9. Time course of MTSET modification. Currents were measured at the end of the test pulse. Monoexponential fits are superimposed (red lines). (A) Time course of MTSET modification of the G163C mutant. (B) Time course of MTSET modification of the R165C mutant. (C) Time course of MTSET modification of the R174C mutant. (D) Time course of MTSET modification of the R176C mutant. (E) Time course of MTSET modification of the R177C mutant. Notice that in this case only closed channels are modified by MTSET. (F) Time course of MTSET modification of the S179C mutant. Only closed channels are modified by MTSET. (G) Mutant L181C was insensitive to the MTSET treatment in both closed and open/closed states.

tively). The second order rate constants obtained from the monoexponential fits of the current-exposure MTSET data for these mutants are shown in Table I. Cysteines 177 and 179 can react with MTSET in closed channels but in closed/open channels these cysteines are not accessible (NA in Table I) to the thiol reagent (Fig. 9, E and F). External MTSET did not modify either closed or closed/open L181C channels (Fig. 9 G). For closed channels, cysteine exposure decreases as we move closer to the COOH-terminal end of S4. For example, cysteine 165 is ~7 times more reactive than cysteine 179 to external MTSET in the closed state. Altogether, these results suggest that when
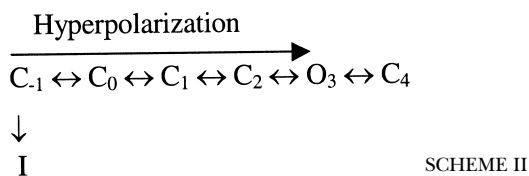
channels open, the S4 segment is displaced inwardly through the plane of the membrane making cysteines 177 and 179 inaccessible to external MTSET.

DISCUSSION

Hoshi (1995), Zei and Aldrich (1998), and Tang et al. (2000) noticed that KAT1 macroscopic currents follow a sigmoidal time curve as predicted by linear models with multiple closed states. The main characteristics of the single-channel and macroscopic currents are well described by the kinetic scheme I shown below (Zei and Aldrich, 1998):

$$\overset{\text{Hyperpolarization}}{\underset{}{\xrightarrow{\hspace{3cm}}}}$$
$$C_0 \leftrightarrow C_1 \leftrightarrow C_2 \leftrightarrow O_3 \leftrightarrow C_4$$
$$\downarrow$$
$$I \hspace{4cm} \text{SCHEME I}$$

Where C indicates closed states, O the open state, and I the inactivated state. The inactivated state that emerges from the deepest closed state was postulated on the basis of first latency plots. On one hand, these plots do not reach a steady-state probability of one (meaning that you find single-channel current records with no openings; blank records) and the inactivated state communicates directly with a closed state. On the other hand, the fact that blank records appear only at depolarized voltages indicates that the transition to the inactivated state takes place from a closed state far from the open state along the activation pathway. A closed state (C_4) after the open state (O_3) is necessary since a closed state starts being populated at large hyperpolarizing voltages. This state is visualized in the single-channel current records as an increase in channel flickering as the voltage is made more negative with the consequent shortening of the mean open time. Our gating current results indicate that a new closed state (C_{-1}) toward the left of C_0 in scheme I is necessary to explain the fast charge movement that develops in the microsecond range, i.e.,

$$\overset{\text{Hyperpolarization}}{\underset{}{\xrightarrow{\hspace{3cm}}}}$$
$$C_{-1} \leftrightarrow C_0 \leftrightarrow C_1 \leftrightarrow C_2 \leftrightarrow O_3 \leftrightarrow C_4$$
$$\downarrow$$
$$I \hspace{4cm} \text{SCHEME II}$$

Most probably, the gating charge measured in our experiments mainly represents charge moved between states C_{-1} and C_0 (fast component) and C_0 and C_1 (slow component) because even during a 30-ms pulse with the largest negative potentials applied, the C_2 state is hardly visited. The slow component of the I_{gON} relaxes with a time constant of 4.2 ms and represents a significant fraction of the total gating charge movement at

−180 mV (65%). This time constant is similar to the one obtained from the rate constants reported by Zei and Aldrich (1998) for the transition between states C_0 and C_1 (∼14 ms) and further supports our contention that the slow gating charge is charge displaced between C_0 and C_1. It is important to note here that the gating current results also show that the voltage sensors are not moving according to a simple resting-activated model, rather they transit between several conformational states during activation of channel by voltage. Thus, KAT1 channel activation is more similar to that found for *Shaker* channels than the one proposed for mSlo channels (compare Baker et al., 1998 and Horrigan and Aldrich, 1999). At present, it is unclear how tight the coupling between the KAT1 channel gate and the voltage sensors is. Our limiting slope determinations, however, show that the gating charge is undiminished even when P_0 reaches values near 10^{-4}. Thus, as in *Shaker* voltage-gated channel, the channel gate appears to be coupled tightly to the voltage sensors.

The results presented here show that the KAT1 channel-forming protein has an intrinsic ability of sensing changes in transmembrane voltage, yet are at difference with *Shaker* channels as it opens when the S4 domain moves inwardly. Therefore, the difference between these two channels must reside in the mechanism that couples voltage sensor displacements with channel opening as proposed for KAT1, the hyperpolarization-activated, cyclic nucleotide–gated spHCN, and MVP, a methanoccocal voltage–gated K$^+$ channel (Cosmelli et al., 2000; Männikö et al., 2002; Latorre et al., 2003; Sesti et al., 2003).

Most of the recent studies ascribe to the S6 α-helices the role of the activation gate. The activation gate would involve a significant separation of the carboxyl termini of the four S6 segments. In particular, structural studies show that the inner helices of the KscA channel line the channel pore and form a bundle crossing near the cytoplasmic side of the channel, leaving an aperture so narrow that it does not allow the passage of ions (Doyle et al. 1998). When activated by protons, these helices are displaced and rotated counterclockwise, increasing the KscA inner aperture and opening the pore (Perozo et al. 1999). The same α-helices play a similar role in a Ca^{2+}-activated K$^+$ channel (MthK) from the *Methanobacterium thermoautotrophicum*. Jiang et al. (2002) proposed that Ca^{2+} binding to its RCK domain pull open the inner α-helices to permit ion conduction. In comparison, the S6 bundle crossing in *Shaker* K$^+$ channels appears to act as a gate that sterically hinders the passage of ions in closed channels (del Camino and Yellen, 2001).

The structure that links the movements of S4 to opening of the activation gate is, however, unknown. Several observations suggest that the S4-S5 linker may be the structure that physically couples the displacements of the S4 with channel opening. HCN channel mutations

of the S4-S5 linker hindered channel closure, suggesting that the structures coupling voltage-sensing elements and channel activation were disrupted (Chen et al., 2001). Mutations in the S4-S5 linker modify the activation gating kinetics in Kv2.1 and Kv3.1 channels (Shieh et al., 1997) and a single mutation (D540) in the S4-S5 linker of HERG produces channels that open with depolarizing and hyperpolarizing voltages (Sanguinetti and Xu, 1999; Tristani-Firouzi et al., 2002). Moreover, chimeric channels constructed using KAT1 and a *Xenopus* depolarization-activated K^{+} channel show that the major determinant for inward rectification resides in the NH$_2$-terminal region of KAT1 that ends in the COOH-terminal of the S4-S5 linker (Cao et al., 1995).

Recent reports (Espinosa et al., 2001; Lu et al., 2001, 2002; Tristani-Firouzi et al., 2002) have revealed complementary sequences in *Shaker* and HERG K^{+} channels essential for coupling the voltage sensor to the activation gate. In *Shaker,* a mismatch between the distal portion of the S4-S5 linker and the carboxy-terminal end of S6 produces voltage-independent channels (Lu et al., 2002). In HERG channels one charged residue (Asp540) in the S4-S5 linker appears to interact electrostatically with Arg665 in the COOH-terminal end of S6 keeping channels shut at hyperpolarized voltages (Tristani-Firouzi et al., 2002). These results suggest that the S4-S5 linker is in direct contact with COOH-terminal end of the S6 segment but important interactions between S5 and S6 segments cannot be discarded at present (e.g., Espinosa et al., 2001). Therefore, we can imagine a mechanism in which the S4 movement depending on voltage polarity will push or pull the S4-S5 linker, displacing and/or rotating the S6 segment to open or close the channel. Indeed, Jiang et al. (2003a,b), on the basis of the crystal structure of a depolarization-gated K^{+} (KvAP) channel, have proposed that the gating charges are carried in an helix-turn-helix structure formed by a stretch of S3 (S3b) and S4, a structure dubbed "the paddle". According to this proposal, during KvAP channel activation, the paddles undergo a displacement of ∼2 nm, which in turn opens the pore by pulling on the S4-S5 linker. If the crystal structure of KAT1 is similar to that of KvAP, channel activation should be controlled by a mechanism in which the channel opens by moving the paddles in reverse. In the lack of a definitive structure for this plant channel, however, it is unclear at present how this movement can open the channel in the case of KAT1.

REFERENCES

Aggarwal, S.K., and R. MacKinnon. 1996. Contribution of the S4 segment to gating charge in the *Shaker* K^{+} channel. *Neuron.* 16: 1169–1177.

Akabas, M.H., D.A. Stauffer, M. Xu, and A. Karlin. 1992. Acetylcholine receptor channel structure probed in cysteine-substitution mutants. *Science.* 258:307–310.

Almers, W. 1978. Gating currents and charge movements in excitable membranes. *Rev. Physiol. Biochem. Pharmacol.* 82:96–190.

Anderson, J.A., S.S. Huprikar, L.V. Kochian, W.J. Lucas, and R.F. Gaber. 1992. Functional expression of a probable *Arabidopsis thaliana* potassium channel in *Saccharomyces cereviciae. Proc. Natl. Acad. Sci. USA.* 89:3736–3740.

Baker, O.S., H.P. Larsson, L.M. Mannuzzu, and E.Y. Isacoff. 1998. Three transmembrane conformations and sequence-dependent displacement of the S4 domain in Shaker K^{+} channel gating. *Neuron.* 20:1283–1294.

Bezanilla, F. 2000. The voltage sensor in voltage-dependent ion channels. *Physiol. Rev.* 80:555–592.

Cao, Y., N.M. Crawford, and J.I. Schroeder. 1995. Amino terminus and the first four membrane-spanning segments of the *Arabidopsis* K^{+} channel KAT1 confer inward-rectification property of plant-animal chimeric channels. *J. Biol. Chem.* 270:17697–17701.

Schoppa, N.E., and F.J. Sigworth. 1998. Activation of shaker potassium channels. I. Characterization of voltage-dependent transitions. *J. Gen. Physiol.* 111:271–294.

Chen, J., J.S. Mitcheson, M. Tristani-Firouzi, M. Lin, and M.C. Sanguinetti. 2001. The S4-S5 linker couples voltage sensing and activation of pacemakers channels. *Proc. Natl. Acad. Sci. USA.* 98: 11277–11282.

Cherel, I., P. Daram, F. Gaymard, C. Horeau, J.-B. Thibaud, and H. Sentenac. 1996. Plant K^{+} channels: structure, activity and function. *Biochem. Soc. Trans.* 24:964–970.

Cosmelli, D., E. Rosenmann, C. Basso, O. Alvarez, and R. Latorre. 2000. The inward rectifier K^{+} channel, Kat1, from *Arabidopsis thaliana* possesses an intrinsic voltage sensor. *J. Physiol.* 523:6P–7P.

del Camino, D., and G. Yellen. 2001. Tight steric closure at the intracellular activation gate of a voltage-gated K^{+} channel. *Neuron.* 32:649–656.

Doyle, D.A., J.M. Cabral, R.A. Pfuetzner, A. Kuo, J.M. Gulbis, S.L. Cohen, B.T. Chait, and R. MacKinnon. 1998. The structure of the potassium channel: molecular basis of K^{+} conduction and selectivity. *Science.* 280:69–81.

Espinosa, F., R. Fleichhauer, A. McMahon, and R.H. Joho. 2001. Dynamic interactions between S5 and S6 during voltage-controlled gating in a potassium channel. *J. Gen. Physiol.* 118:157–169.

Gonzalez, C., E. Rosenman, F. Bezanilla, O. Alvarez, and R. Latorre. 2000. Modulation of the *Shaker* K^{+} channel gating kinetics by the S3-S4 linker. *J. Gen. Physiol.* 115:193–207.

Gonzalez, C., E. Rosenmann, F. Bezanilla, O. Alvarez, and R. Latorre. 2001. Periodic perturbation in *Shaker* K^{+} channel gating kinetics by deletions in the S3-S4 linker. *Proc. Natl. Acad. Sci. USA.* 98:9617–9623.

Hedrich, R., O. Moran, F. Conti, H. Busch, D. Becker, F. Gambale, I. Dreyer, A. Kuch, K. Neuwinger, and K. Palme. 1995. Inward rectifier potassium channels in plants differ from their animal counterparts in response to voltage and channel modulators.

Eur. Biophys. J. 24:107–115.

Horrigan, F.T., and R.W. Aldrich. 1999. Allosteric voltage gating of potassium channels II. m*Slo* channel gating charge movement in the absence of Ca^{2+}. *J. Gen. Physiol.* 114:305–336.

Horrigan, F., and R.W. Aldrich. 2002. Coupling between voltage sensor activation, Ca^{2+} binding and channel opening in large conductance (BK) potassium channels. *J. Gen. Physiol.* 120:267–305.

Hoshi, T. 1995. Regulation of voltage dependence of the KAT1 channel by intracellular factors. *J. Gen. Physiol.* 105:309–328.

Hoth, S., I. Dreyer, and R. Hedrich. 1997. Mutational analysis of functional domains within plant K^+ uptake channels. *J. Exp. Bot.* 48:415–420.

Jiang, Y., A. Lee, J. Chen, M. Cadene, B.T. Chait, and R. MacKinnon. 2002. Crystal structure and mechanism of a calcium-gated potassium channel. *Nature.* 417:515–522.

Jiang, Y., A. Lee, J. Chen, V. Ruta, M. Cadene, B.T. Chait, and R. MacKinnon. 2003a. X-ray structure of a voltage-dependent K^+ channel. *Nature.* 423:33–41.

Jiang, Y., V. Ruta, J. Chen, A. Lee, and R. MacKinnon. 2003b. The principle of gating movement in a voltage-dependent K^+ channel. *Nature.* 423:42–49.

Karlin, A., and M.H. Akabas. 1998. Substituted cysteine accessibility method. *Methods Enzymol.* 293:123–145.

Larsson, H.P., O.S. Baker, D.S. Dhillon, and E.Y. Isacoff. 1996. Transmembrane movement of the *Shaker* K^+ channel S4. *Neuron.* 16:387–397.

Latorre, R., C. Basso, C. Gonzalez, O. Alvarez, and D. Cosmelli. 2001. KAT1, A potassium channel from *Arabidopsis thaliana,* possesses an intrinsic voltage sensor. *Biophys. J.* 80:436a.

Latorre, R., F. Muñoz, C. Gonzalez, and D. Cosmelli. 2003. Structure and function of potassium channels in plants: some inferences about the molecular origin of inward rectification in KAT1 channels. *Mol. Membr. Biol.* 20:19–25.

Lu, Z., A.M. Klen, and Y. Ramu. 2001. Ion conduction pore is conserved among potassium channels. *Nature.* 413:809–813.

Lu, Z., A.M. Klen, and Y. Ramu. 2002. Coupling between voltage sensors and activation gate in voltage-gated K^+ channels. *J. Gen. Physiol.* 120:663–676.

Maatuis, F.J.M., A.M. Ichida, D. Sanders, and J.I. Schroeder. 1997. Roles of higher plant K^+ channels. *Plant Physiol.* 114:1141–1149.

Männikö, R., F. Elinder, and H.P. Larsson. 2002. Voltage-sensing mechanism is conserved among ion channels gated by opposite voltages. *Nature.* 419:837–841.

Mannuzzu, L.M., M.M. Moronne, and E.Y. Isacoff. 1996. Direct physical measure of conformational rearrangement underlying potassium channel gating. *Science.* 271:213–216.

Marten, I., and T. Hoshi. 1998. The N-terminus of the K channel KAT1 controls its voltage-dependent gating by altering the membrane field. *Biophys. J.* 74:2953–2962.

Noceti, F., P. Baldelli, X. Wei, N. Qin, L. Toro, L. Birnbaumer, and E. Stefani. 1996. Effective gating charges per channel in voltage-dependent K^+ and Ca^{2+} channels. *J. Gen. Physiol.* 108:143–155.

Perozo, E., D.M. Cortes, and L.G. Cuello. 1999. Structural rearrangements underlying K^+ channel activation gating. *Science.* 285:73–78.

Sanguinetti, M.C., and Q.P. Xu. 1999. Mutations in the S4-S5 linker alter activation properties of HERG potassium channels expressed in *Xenopus* oocytes. *J. Physiol.* 514:667–675.

Sato, Y., M. Sakaguchi, S. Goshima, T. Nakamura, and N. Uozumi. 2003. Molecular Dissection of the contribution of negatively and positively charged residues in S2-S3, and S4 to final membrane topology of the voltage sensor in the K^+ channel, KAT1. *J. Biol. Chem.* 278:13227–13234.

Sentenac, H., N. Bonneaud, M. Minet, F. Lacroute, J.-M. Salmon, F. Gaymard, and C. Grignon. 1992. Cloning and expression in yeast of a plant potassium ion transporting system. *Science.* 256:663–665.

Schachtman, D.P., J.I. Schroeder, W.J. Lucas, J.A. Anderson, and R.F. Gaber. 1992. Expression of an inward-rectifying potassium channel by the *Arabidopsis KAT1* cDNA. *Science.* 258:1654–1658.

Schonherr, R., and S. Heinemann. 1996. Molecular determinants for activation and inactivation of HERG, a human inward rectifier potassium channel. *J. Physiol.* 493:635–642.

Seoh, S.-A., D. Sigg, D.M. Papazian, and F. Bezanilla. 1996. Voltage-sensing residues in the S2 and S4 segments of the *Shaker* K^+ channel. *Neuron.* 16:1159–1167.

Sesti, F., S. Rajan, R. Gonzalez-Colaso, N. Nokolaeva, and S.A.N. Goldstein. 2003. Hyperpolarization moves S4 sensors inward to open MVP, a methanococcal voltage-gated potassium channel. *Nat. Neurosci.* 6:353–361.

Shieh, C.C., K.G. Klemic, and G.E. Kirsch. 1997. Role of transmembrane segment S5 on gating of voltage-dependent K^+ channels. *J. Gen. Physiol.* 109:767–778.

Shih, T.M., and A.L. Goldin. 1997. Topology of the *Shaker* potassium channel probed with hydrophilic epitope insertions. *J. Cell Biol.* 136:1037–1045.

Sigg, D., and F. Bezanilla. 1997. Total charge movement per channel: The relation between gating displacement and the voltage sensitivity of activation. *J. Gen. Physiol.* 109:27–39.

Sigworth, F.J. 1994. Voltage gating of ion channel. *Quart. Revs. Biophys.* 27:1–40.

Smith, P.L., T. Baukrowitz, and G. Yellen. 1996. The inward rectification mechanism of the HERG cardiac potassium channel. *Nature.* 379:833–836.

Starace, D., and F. Bezanilla. 2001. Histidime scanning mutagenesis of basic residues of the S4 segment of *Shaker* K^+ channel. *J. Gen. Physiol.* 117:469–490.

Stefani, E., M. Ottolia, F. Noceti, R. Olcese, M. Wallner, R. Latorre, and L. Toro. 1997. Voltage-controlled gating in large conductance Ca^{2+}-sensitive K^+ channel (hslo). *Proc. Natl. Acad. Sci. USA.* 94:5427–5431.

Taglialatela, M., L. Toro, and E. Stefani. 1992. Novel voltage clamp to record small, fast currents from ion channels expressed in *Xenopus* oocytes. *Biophys. J.* 61:78–82.

Tang, X.D., I. Marten, P. Dietrich, N. Ivashikina, R. Hedrich, and T. Hoshi. 2000. Histidine[118] in the S2-S3 linker specifically controls activation of the KAT1 channel expressed in *Xenopus* oocytes. *Biophys. J.* 78:1255–1269.

Tristani-Firouzi, M., J. Chen, and M.C. Sanguinetti. 2002. Interaction between S4-S5 linker and S6 transmembrane domain modulate gating in HERG K^+ channels. *J. Biol. Chem.* 277:18894–19000.

Uozomi, N., T. Nakamura, J.I. Schroeder, and S. Muto. 1998. Determination of the transmembrane topology of an inward-rectifying potassium channel from *Arabidopsis thaliana* based on functional expression in *Escherichia coli. Proc. Natl. Acad. Sci. USA.* 95:9773–9778.

Urbach, S., I. Cherel, H. Sentenac, and F. Gaymard. 2000. Biochemical characterization of the *Arabidopsis* K+ channels KAT1 and AKT1 expressed or co-expressed in insect cells. *Plant J.* 23: 527–538.

Yang, N., and R. Horn. 1995. Evidence for voltage-dependent S4 movement in sodium channels. *Neuron.* 15:213–218.

Yang, N., A.L. George, and R. Horn. 1996. Molecular basis of charge movement in voltage-Gated sodium channels. *Neuron.* 16:113–122.

Yellen, G. 1998. The moving parts of voltage-gated ion channels. *Quarterly Reviews of Biophysics.* 31:239–295.

Zagotta, W.N., T. Hoshi, J. Dittman, and R.W. Aldrich. 1994. Shaker potassium channel gating. II: Transitions in the activation pathway. *J. Gen. Physiol.* 103:279–319.

Zei, P.C., and R.W. Aldrich. 1998. Voltage-dependent gating of single wild-type and S4 mutant KAT1 inward rectifier potassium channels. *J. Gen. Physiol.* 112:679–713.